

## Multi-parameter estimating photometric redshifts with artificial neural networks

Lili Li<sup>1,2</sup>, Yanxia Zhang<sup>1</sup>, Yongheng Zhao<sup>1</sup> and Dawei Yang<sup>2</sup>

1. National Astronomical Observatories, Chinese Academy of Sciences, China, 2. College of Physics  
 Science and Information Engineering, Hebei Normal University, Shijiazhuang,

**Abstract** We calculate photometric redshifts from the Sloan Digital Sky Survey Data Release 2 Galaxy Sample using artificial neural networks (ANNs). Different input patterns based on various parameters (e.g. magnitude, color index, flux information) are explored and their performances for redshift prediction are compared. For ANN technique, any parameter may be easily incorporated as input, but our results indicate that using reddening magnitude produces photometric redshift accuracies often better than the Petrosian magnitude or model magnitude. Similarly, the model magnitude is also superior to Petrosian magnitude. In addition, ANNs also show better performance when the more effective parameters increase in the training set. Finally, the method is tested on a sample of 79, 346 galaxies from the SDSS DR2. When using 19 parameters based on the reddening magnitude, the rms error in redshift estimation is  $\sigma_z = 0.020184$ . The ANN is highly competitive tool when compared with traditional template-fitting methods where a large and representative training set is available.

**Key words:** galaxies: fundamental parameters — techniques: photometric — method: data analysis

### 1 INTRODUCTION

Photometric redshifts refer to the redshift estimation of galaxies using only medium- or broad-band photometry or imaging instead of spectroscopy. There is a fact that broad band photometry is on the order of magnitudes less time consuming than spectroscopy. Furthermore, photometry is available for faint galaxies that are not spectroscopically accessible, at the least, because of finite telescope time. In addition, a greater area of the sky covered by imaging detectors usually makes the redshifts of more objects measured simultaneously than by spectroscopy that is only limited to individual galaxies or those positioned on slits or fibres. The importance of the technique is growing not only with the desire to gain a greater understanding of galaxy evolution (for example, the determination of luminosity function), but also in weak gravitational lensing, where redshift estimates can reduce contamination from intrinsic alignments (Heymans & Heavens 2003; King & Schneider 2003). If the method can be found to obtain an accurate estimate of the redshift for the larger photometric catalog, much better constraints on the formation and evolution of large-scale structural elements such as galaxy cluster, filaments, and cosmological models (e.g. Blake & Bridle 2005) in general may be achieved. However, photometric redshifts subject to relatively lesser precision. For many applications such as determining properties of large numbers of galaxies and the large-scale structure of the universe, it is quite tolerable and sometimes even more effective.

The concept of photometric redshifts was first developed by Baum (1962). Since then, many new methods have been applied to calibrate photometric-redshift relations. To date, these methods have typically been employed on multicolor deep-field and wide-field surveys, notably the Hubble Deep Field (e.g. Gwyn & Hartwick 1996; Sawicki et al. 1997; Connolly et al. 1998; Fernández-Soto et al. 1999; Fontana et al.

\* E-mail: lily@lamost.org

2000; Vanzella et al. 2004; Coe et al. 2006) and the Sloan Digital Sky Survey (Sowards-Emmerd et al. 2000; Casbaj et al. 2003; Weinstein et al. 2004). The most common way of estimating photometric redshifts is the template-matching technique. It requires to convert the photometric data of each galaxy into spectral energy distribution (SED) and compile a library of template spectra covering galaxy types, luminosities and redshifts in the range of interest. For a particular target galaxy, the photometric redshift is selected to be the redshift of the most closely matching template spectrum; This is usually defined by minimizing the  $\chi^2$  between the template and actual magnitudes. The template-matching photometric redshift technique makes use of the available and reasonably detailed knowledge of galaxy SED and in principle it may be used reliably even for populations of galaxies with few or no spectroscopically confirmed redshifts. However, its success strongly depends on the compilation of a library of accurate and representative template SEDs (see e.g. Hogg et al. 1998). In the situation with a large amount of prior redshift information about the sample, the template-matching technique is not the best approach.

An alternative approach is a polynomial or other function fitting, mapping the photometric data to the known redshifts and using this to estimate redshifts for the remainder of the sample with unknown redshifts (e.g. Sowards-Emmerd et al. 1999). In essence, its aim is to derive a parametrization for the redshift as a function of photometric parameters. This requires a large and representative training set of galaxies with both photometry and a precisely known redshift. A simple example is to express the redshift as a polynomial in the galaxy colours (Connolly et al. 1995; Sowards-Emmerd et al. 2000). The coefficients in the polynomial are varied to optimize the fit between the predicted and measured redshift. The photometric redshifts for galaxies with unknown spectroscopy can then be estimated by utilizing the optimized function to the colours of the target galaxy.

In the recent years, a variety of techniques to estimate photometric redshifts have emerged based on machine learning. Artificial neural networks (ANNs) as a new possibility among the interpolative techniques have been used in astronomy. Popular applications include: star/galaxy separation (e.g. Odewahn & Nielsen 1994; Bertin & Arnouts 1996; ), morphological classification of galaxies (Nievius & Odewahn 1994; Lahav et al. 1996; Ball et al. 2004), spectral classification (Folkes et al. 1996; Weaver 2000). Certainly, ANNs have also been applied for the photometric redshift prediction (Tagliaferri et al. 2002; Firth et al. 2003; Ball et al. 2004; Vanzella et al. 2004; Collister & Lahav 2004).

ANNs are applicable to ‘mixed’ data sets in which a moderately large training set with photometry in the survey filters and spectroscopic redshifts for the same objects are available. The generality of using ANN method is that any parameter can be used to train the network and make out prediction, hence photometric redshifts can be obtained. In practice, one can measure an almost limitless number of parameters to describe a galaxy. However, it is desirable to have as much information as possible in the fewest parameters, either continuous or discrete. The fewer parameters should be physically meaningful, i.e. they should be directly predicted by theories of galaxy and large scale structure formation, or be related in a quantitative way. Hence, it is necessary to find out what parameters are the most helpful and useful for photometric redshift evaluation.

The paper explores the use of ANNs as a potential tool for photometric redshift determination. Mainly we focus on establishing the best set of parameters and compare the effect of different input parameter sets on redshift estimation. The layout of this paper is as follows. In section 2 the principle of ANNs is introduced. Section 3 describes the data in detail and parameters used in the experiments. The procedure to estimate redshifts with different parameter sets is presented in Section 4. In Section 5 the performances of different parameter sets are discussed and the conclusion is given in Section 6.

## 2 ARTIFICIAL NEURAL NETWORKS

ANNs, being originally conceived as models of the brain, are collections of interconnected neurons each able to carry out simple processing. Artificial neural networks are composed of massively parallel distributed processors that have a natural property for storing experiential knowledge and making it available for use. The knowledge is acquired by the network through a learning process and interneuron connection strengths - known as synaptic weights - are used to store the knowledge (Haykin 1994).

The practical applications of ANNs most often employ supervised learning. For supervised learning, you must provide training data that includes both the input (a set of vectors of parameters, here each vector

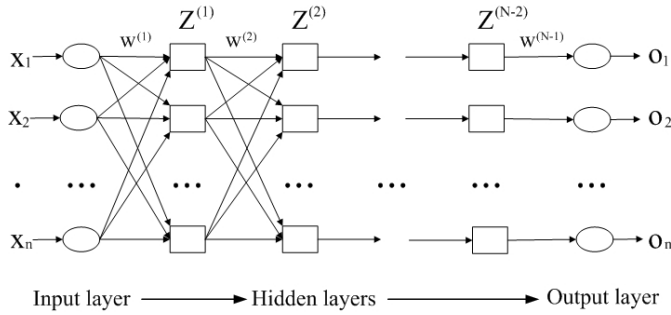


**Fig. 1** A schematic diagram of neural network structure. The ANNs with input nodes taking, for example, magnitudes in various filters, the middle hidden layers, and a single output node giving, for example, redshift  $z$ . Each connecting line carries a weight  $w_{ij}$ .

representing a galaxy) and the desired result or the target value (the corresponding redshifts). After the network is trained successfully, you can present input data alone to the ANNs (that is, input data without the desired result), and the ANNs will compute an output value that approximates the desired result.

This is achieved by using a training algorithm to minimize cost function which represents the difference (error) between the actual and desired output. The cost function  $E$  is commonly of the form

$$E = \frac{1}{p} \sum_{k=1}^p (o_k - t_k)^2 \quad (1)$$

where  $o_k$  and  $t_k$  are the output and target respectively for the objects.  $p$  represents the number of samples. Generally the topology of ANNs can be schematized as a set of  $N$  layer (see Fig.1), each layer being composed by neurons. The first layer ( $i = 1$ ) is usually called ‘input layer’, the intermediate ones ‘hidden layers’ and the last one ( $i = N$ ) ‘output layer’. Each neuron  $j$  in the  $s$  layer derives a weighted sum of the  $M$  output  $z_i^{(s-1)}$  from the previous layer ( $s - 1$ ) and, through either a linear or a non-linear function, produces an output,

$$z_j^{(s)} = f \left( \sum_{i=0}^M (w_{ji}^{(s)} z_i^{(s-1)}) \right) \quad (2)$$

Note that  $w_{j0}$  denotes the bias for the hidden unit  $j$ , and  $f$  is an activation function such as the continuous sigmoid or, as used here, the tanh function, which has an output range of -1 to 1:

$$f(x) = \frac{2}{1 + e^{-2x}} - 1 \quad (3)$$

When the entire network has been executed, the outputs of the last layer act as the output of the entire network. The free parameters of ANNs are weighted vectors. During training neural networks, the weights of connections are adjusted on the basis of data to minimize the total error function. The learning procedure is the so called ‘back propagation’. The number of layers, the number of neurons in each layer, and the functions are chosen from the beginning and specify the so called ‘architecture’ of the ANNs.

Neural networks learn by example. The neural network user gathers representative data as a training set and initiates the weight vector with a random seed, then invokes training algorithms to automatically learn the structure of the data. Here we use a popular algorithm in neural net research: the Levenberg-Marquardt method (Levenberg 1944; Marquardt 1963, also detailed in Bishop 1995). This has the advantage that it is very quick to converge to a minimum of the error function that may not have just a global minimum in the multidimensional weight space but could have a number of local minima instead. In any case, networks

trained using the exact same training set for the same number of epochs but using different initial weights (and therefore different starting points in this space) will converge to slightly different final weights.

In order to avoid (possible) over-fitting during the training, another part of the data can be reserved as a validation set (independent both of the training and test sets, not used for updating the weights), and used during the training to monitor the generalization error. After a chosen number of training iterations, training terminates and the final weights chosen for the ANN are those from the iteration at which the cost function is minimal on the validation set. It is called so ‘early stopping method’. This is useful to avoid over-fitting to the training set if the training set is small. But the disadvantage of this technique is that it reduces the amount of data available for both training and validation, which is particularly undesirable if the data set is small.

### 3 CHOSEN GALAXY SAMPLE AND PARAMETERS

The SDSS consortium has publicly released more than  $10^5$  spectroscopic galaxy redshifts in the Data Release 2 (DR2). In order to test the accuracy of the photometric redshifts derived from SDSS DR2, we selected all objects satisfying the following criteria (also see Vanzella et al. 2004): (1)  $r$ -band Petrosian magnitude  $r < 17.77$ ; (2) the spectroscopic redshift confidence must be greater than 0.95 and there must be no warning flags. This gave 159 346 galaxies, which are randomly partitioned into training, validation and test sets with respective sizes 60 000, 20 000 and 79 346. We will explore different network complexities, the validation set is required to compare them, and the test set is used at the end to estimate the true error of final network.

With different magnitude measurements given by SDSS, we compare the effect of parameters for predicting redshift and give the input patterns of many different parameter sets, which mainly include Petrosian magnitudes, model magnitudes and reddening magnitudes in five different bands. The Petrosian (1976) magnitude is based on the flux within an aperture defined by the ratio of the local surface brightness to the mean interior surface brightness. The model magnitude is used as a template to determine PSF magnitude in each band. The galaxy images are fitted with the de Vaucouleurs profile and the exponential profile of arbitrary axis ratio and orientation. Each of these fits has a goodness and the total magnitude associated with the better fit of the two models is referred to as the ‘model’ magnitude. The magnitude by reddening correction is named reddening magnitude. One advantage of our ANN approach to photometric redshift estimation is that additional parameters that can help in estimating the redshift can be easily incorporated as extra input pattern. However, these parameters need to be chosen carefully such that they have a genuine dependence on the redshift. Here, we supplemented the 50% and 90% Petrosian flux levels of SDSS training sample as additional inputs to the ANNs. They are the angular radii containing the stated fraction of the Petrosian flux. Each of these radii is a measure of the angular size of the galaxy, which is a redshift-dependent property.

### 4 REDSHIFT PREDICTION WITH DIFFERENT PARAMETER SETS

The experiments were performed using ANNs in the Matlab nnet Toolboxes. The training and test samples are independent, but in fact it is required the training ones are representative of the test ones. The neural network trained on the training set with success can be applied to the test sample with the same generalization and learning ability. During the training, we changed a variety of net architectures and initialized the random distributions of weights to save the ‘best’ distribution that corresponds to the lowest error in training sample (in almost all cases coincident with the last epoch).

In order to evaluate the accuracy of the prediction, we define the variance between the neural outputs ( $z_{\text{NN}}$ ) and the targets (spectral redshift  $z_{\text{spec}}$ ), as below:

$$\sigma_z = \sqrt{\frac{1}{N} \sum_i (z_{\text{NN}} - z_{\text{spec}})^2} \quad (4)$$

where  $N$  is the number of galaxies, and  $i = 1 \dots N$ . That is the statistical estimate for redshift prediction of a given neural network architecture.

**Table 1** the comparison of different sets of parameters using Petrosian magnitude

Input	Parameters	$\sigma_z$ (Train)	$\sigma_z$ (Test)
5	Petro $u, g, r, i, z$	0.026939	0.027031
5	Petro $u - g, g - r, r - i, i - z, r$	0.026535	0.026717
7	Petro $u - g, g - r, r - i, i - z, r$ , PetR50, PetR90	0.025002	0.025131
19	Petro $u - g, g - r, r - i, i - z, u, g, r, i, z$ , PetU50, PetU90, PetG50, PetG90, PetR50, PetR90, PetI50, PetI90, PetZ50, PetZ90	0.021502	0.021596

#### 4.1 Petrosian parameters

In this exploration, we selected the Petrosian magnitudes in five different bands from SDSS DR2 as the root data. The Petrosian magnitude system which measures flux in apertures is determined by the shape of the surface brightness profile. By increasing other parameters or changing different parameter combination as input pattern, the neural networks were trained and the final testing results were assessed with the Eq.4.

In this experiment, we directly used the Petrosian magnitudes in five bands ( $u, g, r, i, z$ ) as the first set of input parameters for neural networks. The number of hidden units was chosen using trial and error rather a quantitative method, such as the Bayesian information criterion, because there is no one procedure for choosing the number that applies to many datasets which is clearly superior to trial and error. Our training therefore has been carried out using one or two hidden layers and different nodes. The weights corresponding to the minimum training error have been stored. The best resulting error is  $\sigma_z = 0.027031$  with the architecture 5:10:10:1 (five input nodes, two hidden layers with ten and ten units and one output nodes).

To compare the effect of different parameters, we exchanged the color index ( $u - g, g - r, r - i, i - z$ ) and the  $r$ -band magnitude ( $r$ ) as the input of neural net. Combining different architectures with different numbers of units in the hidden layers and selecting the best distribution of weights, the final determined network architecture is 5:10:10:1 and the dispersion in testing set is  $\sigma_z = 0.026717$ . We can see the result is slightly better than the previous experiment. Unfortunately, the accuracy is not adequate for our photometric redshift estimation. So we need to consider increasing some information to solve this problem.

Certainly, there will be more information if more parameters are included, here the  $r$ -band 50 and 90 per cent Petrosian flux radii (PetR50, PetR90) were added as two extra inputs to our ANNs. In this case, there are 7 input parameters as input pattern. By the experimental trial, we choose the ultimate structure is 7:16:16:1 and the rms scatter for this combination in testing set is  $\sigma_z = 0.025048$ . We can see the new information produced some improvement and 7 parameters is preferable to the only five input patterns.

Indeed, increasing information in the training data is an obvious method to improve the generalization. Now let us take the various parameters into account such as the Petrosian 50 and 90 percent flux radii in all bands and the magnitudes in the five different bands. For this experiment, we gave 19 parameters (see Table 1.) and the chosen networks was a single hidden layer with 20 neurons. The experiment shows that increasing the number of nodes in the architecture of neural network does not cause the results to change significantly. The trial final structure is 19:20:1 and the scatter is down to 0.021596. The result shows that correspondingly adds some new information gives a clearly better improvement. We compared the spectroscopic redshifts with the ANN photometric redshifts for our experiment with 19 parameters in Fig.2. The results of dispersion ( $\sigma_z$ ) for each set of parameters to estimate photometric redshifts are summarized in Table 1.

#### 4.2 Model parameters

We have attempted to find the optimal set of parameters to use in a neural network for estimating photometric redshifts, which leaves a nonexpert asking the question ‘how should I decide what parameters to use?’ The comparison process can be customized by specifying additional comparison parameter such as

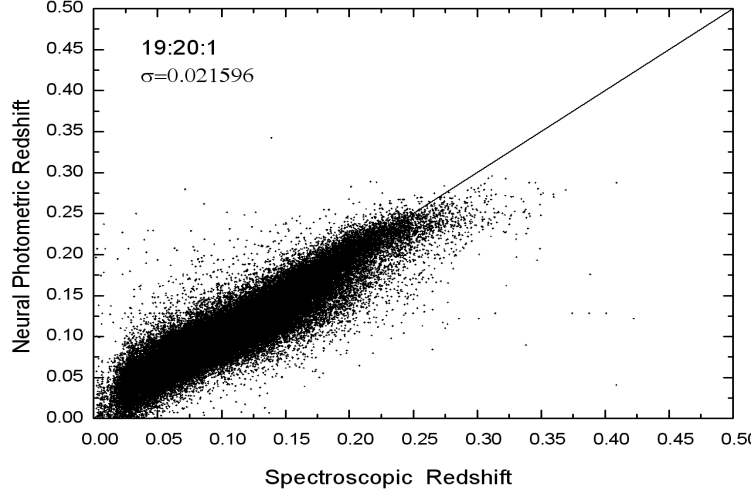


**Fig. 2** the spectroscopic redshifts vs. the photometric redshifts, the redshift prediction in the SDSS DR2 (79, 346 galaxies) sample using 19 Petrosian magnitude parameters. The ANN architecture is 19:20:1 and the scatter is 0.021596

model magnitude. In another experiments, we mainly focus on the model magnitudes in five different bands or some combination with other parameters to make a detailed comparison of different parameters on the same sample.

Firstly, we applied the model magnitudes in five bands ( $u, g, r, i, z$ ) as the input parameters for neural networks. A 5:12:8:1 neural network was trained for 80 epochs with validation set leading early termination and random initialization of the weights is adopted. The network trained by model magnitudes produces a dispersion in testing sample  $\sigma_z = 0.0233$ .

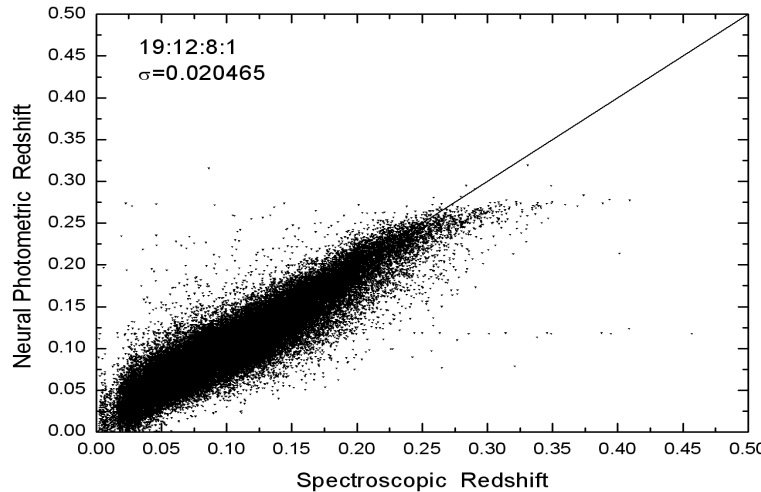
Instead of using only the magnitudes, we took four model color index ( $u - g, g - r, r - i, i - z$ ) and the model magnitude in  $r$  band as input parameters to make comparison with the first one. In this way, we used the same net architecture 5:12:8:1 and varied different distribution of weights. The ultimate prediction error at network output  $\sigma_z = 0.0221$  is relatively small.

As a comparison of the parameters, we also added PetR50 and PetR90 to the above five input patterns like the Petrosian magnitude experiment. A 7:12:8:1 network with initial 3000 epochs, has been carried out by changing the initial random distribution of weights and early stopping to void over-fitting during the training. Many network runs could be used to select good and simple structure. The final error  $\sigma_z = 0.02075$  is remarkably improved. It is comparable to the other photometric redshifts in the literature found using neural networks, e.g. Tagliaferri et al.(2002), Firth, Lahav & Somerville (2003), Vanzella et al.(2004), Collister & Lahav (2004). So employing PetR50 and PetR90 in this process seems to be crucial in improving the agreement between photometric and spectroscopic redshifts.

Finally, we added some new information in the training set in order to reduce the systematic errors. Based on the above parameters, all the model magnitudes and the Petrosian 50 and 90 per cent flux radii in the other bands are considered and together 19 parameters (see Table 2.) are input to the network. By trial, we select network architecture 19:12:8:1 and its dispersion is  $\sigma_z = 0.020465$  which is a slight improvement because of the addition of other parameters. Fig. 3 compares the ANN redshifts with spectroscopic

**Table 2** the comparison of different sets of parameters using model magnitude

Input	Parameters	$\sigma_z$ (Train)	$\sigma_z$ (Test)
5	model $u, g, r, i, z$	0.023354	0.023321
5	model $u - g, g - r, r - i, i - z, r$	0.022006	0.022097
7	model $u - g, g - r, r - i, i - z, r$ , PetR50, PetR90	0.020765	0.02075
19	model $u - g, g - r, r - i, i - z, u, g, r, i, z$ , PetU50, PetU90, PetG50, PetG90, PetR50, PetR90, PetI50, PetI90, PetZ50, PetZ90	0.02034	0.020465

**Fig. 3** A comparison of photometric and spectroscopic redshifts using 19 model magnitude parameters. The ANN architecture 19:12:8:1 is used. The ANNs were tested on a separate testing set of size 79, 346 (plotted) and the result is  $\sigma_z=0.020465$ .

redshifts for a testing set of 79, 346 galaxies with 7:12:8:1 and 19:12:8:1 networks, respectively. In Table 2, we summarized some of the results obtained from the above experiments.

#### 4.3 Reddening magnitude parameters

Similar to the procedure to predict photometric redshifts based on petrosian and model parameters by ANNs, here we discuss the parameter sets based on reddening magnitudes, as well as the dispersion of redshift estimation. In detail, we adopted the same sample and the training has been carried out setting the maximum number of epochs to 3000. Different architectures have been used with one or two hidden layers and different numbers of nodes. For different parameter sets, the ANN architectures are 5:5:5:1, 5:5:10:1, 7:10:1 and 19:12:1, respectively. Correspondingly, the RMS of redshifts is listed in Table 3. The best result of this set of parameters is  $\sigma_z = 0.020184$ , where 19 parameters are considered.

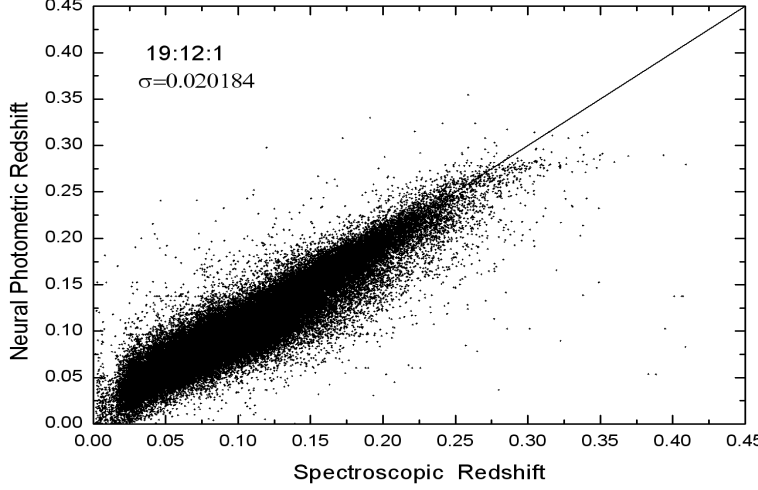


**Fig. 4** Redshifts prediction using reddening magnitude with 19 input parameters. The ANN architecture is 19:12:1 and the testing sample is 79, 346 (plotted).

Moreover, we have studied the effect of adding the error of model magnitude (5 parameters) on redshifts estimation. Here, we give the input patterns of network with 24 parameters, including the above 19 reddening magnitude and 5 model error parameters. Finally, the network produced the scatter  $\sigma_z = 0.020053$ .

**Table 3** the comparison of different sets of parameters using reddening magnitude

input	Parameters	$\sigma_z$ (Train)	$\sigma_z$ (Test)
5	redden $u, g, r, i, z$	0.021371	0.02388
5	redden $u - g, g - r, r - i, i - z, r$	0.021081	0.021097
7	redden $u - g, g - r, r - i, i - z, r$ , PetR50, PetR90	0.020821	0.020689
19	redden $u - g, g - r, r - i, i - z, u, g, r, i, z$ , PetU50, PetU90, PetG50, PetG90, PetR50, PetR90, PetI50, PetI90, PetZ50, PetZ90	0.020174	0.020184

## 5 DISCUSSION

We have presented extensive experiments with a variety of parameters for the estimation of redshifts based on feed-forward neural networks. There are a few things to observe about these results. First, the experiment of Petrosian magnitudes as the root data is listed in Table 1. The combination of four color index with Petrosian magnitude in  $r$  band ( $u - g, g - r, r - i, i - z, r$ ) has better performance than only five magnitudes ( $u, g, r, i, z$ ) for our experiment. Therefore, the second set of parameters will be more suitable for the estimation of photometric redshifts. In order to improve the prediction result and investigate the effect of other parameters, we add PetR50 and PetR90 as input patterns. The result shows that the prediction accuracy of 7 parameters surpassed that with 5 parameters towards the same data. Finally, as shown in Table 1 when 19

parameters are taken, the prediction for redshifts markedly improves and the correspond system error rate also decreases.

Secondly, we transformed the model magnitudes as basic input pattern. It is shown in Table 2 that the second set of parameters has yielded higher prediction accuracy than the first one, namely the performance of the combination of model color index with the magnitude in  $r$  band is better than using only five magnitudes. Likely, we add two other parameters (PetR50, PetR90) which will offer some new information for training. Generally speaking, with the increasing availability of information, the prediction should be continually improved, because of more features considered and more information given. Indeed, the 7 parameters concerning more information about data have a rather good performance. We similarly utilized 19 parameters for the estimation of photometric redshifts and finally compared its scatter with that of the 7 parameters for the same test sample. As shown in Table 2, the result of 19 parameters gave a slight improvement.

Thirdly, The results of using reddening magnitudes parameters for the sample are given in Table 3. Comparing the results, similarly, we can see the combination of four color index with reddening magnitude in  $r$  band ( $u - g, g - r, r - i, i - z, r$ ) is better than only five magnitudes ( $u, g, r, i, z$ ). Moreover, PetR50 and PetR90 as effective parameters also improved the performance of neural network. When 19 parameters are considered, more parameters giving more information, the result of prediction for redshift is also increased.

Finally, as indicated in Table 1-3, when similarly considering the magnitudes in five bands, the reddening magnitudes as parameters obtained a smallest dispersion  $\sigma_z^{test}$  among three kinds of magnitudes and the model magnitude is better than Petrosian magnitude. In addition, all the combinations of parameters for reddening magnitudes are superior to those with Petrosian magnitudes and model magnitudes. Furthermore, there is a slight improvement when we consider the error of model magnitude.

## 6 CONCLUSION

In this paper, we have described experiments comparing the performance of a number of different parameters for estimating photometric redshifts. From the experimental results, we can easily see no matter using the Petrosian magnitude, the model magnitude or the reddening magnitude, there is a common conclusion that the more parameters are considered, the higher the accuracy is. As the parameters increase in the training data, there will be more information for the network to improve its capability of prediction and generalization, so the final accuracy is also advanced correspondingly. Moreover, it is clear that the performance of reddening magnitude is superior to that using Petrosian magnitude or model magnitude for the same parameter structure and the same data set. Therefore, we can see the reddening magnitude offers some significant advantage over the Petrosian magnitude and model magnitude, though the three sets of parameters are available for neural networks to estimate the photometric redshifts. Our best prediction accuracy for photometric redshifts is  $\sigma_z = 0.020184$ , which is the statistical computation of samples covered the area and which will help large-scale structure researchers to easily study some cosmic related issues.

With the advance in astronomical observation, there have been more and more parameters available, it therefore becomes increasing desirable to select the most suitable parameters among them for astronomers to use. This is a major problem for empirical photometric redshift estimation where inappropriate parameters that have no obvious redshift dependence will lead to larger scatter and error. Selecting appropriate and effective parameters is a challenging issue in future research. In order to improve the accuracy of estimating photometric redshifts, we will consider more parameters from multiwavelength band, such as  $J, H, K_s$  from 2MASS. Moreover we will further perform feature extraction (e.g. principal component analysis, PCA) to reveal underlying factors or components in a multi-dimensional parameter space.

The above neural network applications were concerned with the photometric redshift, but neural networks have had wider applications in astronomy. The usefulness of neural networks derives from the fact that they are an efficient and effective means of tackling problems which are non-linear or concerned with multi-parameter problems. Neural network techniques for solving problem are designed primarily to give an accurate representation of the relationship between two sets of variables, and they are particularly successful when the relationship is highly complex. When implemented in estimating redshift process, it becomes evident that neural networks are a very useful and adaptable addition to the tools available to astronomers in tackling a wide variety of problems (i.e. classification, regression, feature selection).

## References

Adams A., Woolley A., 1994, *Vistas in Astronomy*, 273, 280

Ball N.M., Loveday J., Fukugita M. et al., 2004, *MNRAS*, 348, 1038

Baum W. A., 1962, *IAU Symp. No. 15, Problems of Extragalactic Research*, p.390

Bertin E., Arnouts S., 1996, *A&AS*, 117, 393

Blake C., Bridle S., 2005, *MNRAS*, 363, 1329

Bishop C. M., 1995, *Neural Networks for Pattern Recognition*, Oxford University Press

Csabai I., Budavári T., Connolly A. J. et al., 2003, *AJ*, 125, 580

Coe D., Benítez N., Sánchez S. F. et al., 2006, *AJ*, 132, 926

Collister A. A., Lahav O., 2004, *PASP*, 116, 345

Connolly A. J., Csabai I., Szalay A. S., 1995, *AJ*, 110, 2655

Connolly A. J., Szalay A. S., Brunner R. J., 1998, *ApJ*, 499, L125

Fernández-Soto A., Lanzetta K. M., Yahil A., 1999, *ApJ*, 513, 34

Firth A. E., Lahav O., Somerville R. S., 2003, *MNRAS*, 339, 1195

Folkes S. R., Lahav O., Maddox S. J., 1996, *MNRAS*, 283, 651

Fontana A., D'Odorico S., Poli F. et al., 2000, *AJ*, 120, 2206

Gwyn S. D. J., Hartwick F. D. A., 1996, *ApJ*, 468, 77

Haykin S. 1994, *Neural Networks: A Comprehensive Foundation*, Macmillan College Publishing Company

Heymans C., Heavens A., 2003, *MNRAS*, 339, 711

Hogg D. W., Cohen J. G., Blandford R., 1998, *AJ*, 115, 1418

King L. J., Schneider P., 2003, *A&A*, 398, 23

Lahav O., Naim A., Sodré L. J. et al., 1996, *MNRAS*, 283, 207

Levenberg K., 1994, *Quarterly Journal of Applied MathematicII*, 2, 164

Marquardt D.W., 1963, *Journal of the Society of Industrial and Applied Mathematics*, 11, 431

Nielsen M. L., Odewahn S. C., 1994, 185th AAS Meeting, 26, 1498

Odewahn S. C., Nielsen M. L., 1994, *Vistas in Astronomy*, 38, 281

Sawicki M. J., Lin H., Yee H. K. C., 1997, *Proceedings of the 37th Herstmonceux conference*, p.175

Sowards-Emmerd D., McKay T. A., Sheldon E. et al., 1999, *American Astronomical Society*, 31, 827

Sowards-Emmerd D., Smith J. A., McKay T. A. et al., 2000, *AJ*, 119, 2598

Tagliaferri R., Longo G., Andreon S. et al., 2002, *astro-ph/0203445*

Vanzella E., Cristiani S., Fontana A. et al., 2004, *A&A*, 423, 761

Wadadekar Y., 2005, *PASP*, 117, 79

Weaver W. B., 2000, *ApJ*, 541, 298

Weinstein M. A., Richards G. T., Schneider D. P. et al., 2004, *ApJS*, 155, 243

York D. G., Adelman J., Anderson J. E. et al., 2000, *AJ*, 120, 1579